Accepted Manuscript

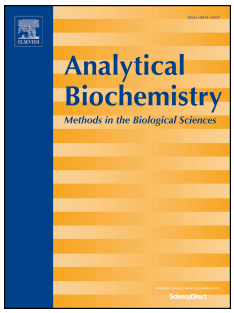

Label-free and simple detection of endotoxins using a sensitive LSPR biosensor based on silver nanocolumns

Mohamad Zandieh, Seyyed Nezam Hosseini, Manouchehr Vossoughi, Maryam Khatami, Sara Abbasian, Ahmad Moshaii

PII: S0003-2697(18)30193-3

DOI: 10.1016/j.ab.2018.02.023

Reference: YABIO 12947

To appear in: *Analytical Biochemistry*

Received Date: 1 January 2018

Revised Date: 22 February 2018

Accepted Date: 23 February 2018

Please cite this article as: M. Zandieh, S.N. Hosseini, M. Vossoughi, M. Khatami, S. Abbasian, A. Moshaii, Label-free and simple detection of endotoxins using a sensitive LSPR biosensor based on silver nanocolumns, *Analytical Biochemistry* (2018), doi: 10.1016/j.ab.2018.02.023.

Label-Free and Simple Detection of Endotoxins Using a Sensitive LSPR Biosensor Based on Silver Nanocolumns

Mohamad Zandieh, Seyyed Nezam Hosseini*, ManouchehrVossoughi, Maryam Khatami, Sara Abbasian and Ahmad Moshaii.

This paper describes the construction of a silver-based LSPR biosensor for endotoxin detection. We used GLAD method to procure reproducible silver nanocolumns. In this work, the silver nanostructures were considerably stabilized by a SAM of MPA, and the limit of detection of biosensor was measured to be 340 pg/ml for endotoxin *E.coli*. Considering endotoxin *B.abortus* as the second type of endotoxin contamination in our target samples (HBs-ag produced in Institute Pasteur, Iran), we investigated selectivity of the biosensor in various experiments. We showed that this biosensor can selectively detect both types of endotoxins compared to other biological species. Overall, this study proposes that LSPR biosensing can be considered as a sensitive, simple, and label-free method for endotoxin detection in the quality control laboratories.

Keywords: LSPR Biosensor, Endotoxin, Label-Free, Silver Nanocolumns, GLAD Method

Abbreviations: LSPR; Localized Surface Plasmon Resonance, GLAD; Glancing Angle Deposition, SAM; Self Assembled Monolayer, MPA; Mercaptopropionic Acid.

Introduction

Lipopolysaccharide (LPS), also known as endotoxin, is a highly toxic component that exists in the outer membrane of gram negative bacteria. It is released into the environment during every phase of bacterial growth cycle(1), so it causes contamination of a wide range of biopharmaceutical products. Even small quantities of endotoxin injected to human body can result in fever, septic shock, and death(2). Therefore, it is highly important to detect and also quantify endotoxin of biopharmaceutical products in quality control laboratories. The most validated method used for endotoxin detection is Limulus Amebocyte Lysate (LAL) test. Although this method is sensitive, it has some unavoidable drawbacks such as highly dependency on temperature, long incubation times to access the results, hard multistep preparation procedures and being expensive(3). These problems forced research groups all around the world into working on novel methods of endotoxin detection based on biosensors.

Biosensing is a process in which a biological element interacts with an analyte, and then the result of the interaction is sent to a transducer as a response. There are several published papers which used biosensors for endotoxin detection. The researchers have used all the electrochemical (4-16), optical (3, 17-21) and mass-based(22) approaches of biosensing. Biosensor miniaturizing, improving sensitivity, lowering expenses and increasing simplicity are the most important objectives that have been investigated by these researchers. In order to reach these objectives, we suggested using an LSPR biosensor for endotoxin detection.

In recent years, LSPR biosensors are gaining importance due to their interesting detection characteristics. LSPR is a hallmark of noble metal nanoparticles that caused by collective oscillation of the conduction electrons at nanoparticles surface. In LSPR biosensors, interaction of biomolecules at the surface of sensor leads to a change in the refractive index of surrounding medium. As a result, a change occurs in the LSPR peak wavelength of the extinction spectra. Therefore, the wavelength shift ($\Delta\lambda_{max}$) represents the detection of analytes in these biosensors.

In this paper, we constructed an LSPR biosensor based on silver nanocolumns for detection of endotoxin. For deposition of silver nanocolumns, we used GLAD method due to its low cost and ability to control shape of nanoparticles (23). In addition, as expected, nanostructures produced by this method are notably reproducible. A polycationic peptide, Polymyxin B (PmB), has been used as a biorecognition element to interact with endotoxin. We chose PmB, because it is more stable, more homogeneous, and less expensive (˜2000*less) than other conventional peptides and aptamers used as biosensing element(7,24). Moreover, due to its high positive charge, PmB has considerable affinity to endotoxin molecules and can neutralize endotoxin toxicity. SAMs of MPA and EDC-NHS was performed on the surface of silver nanoparticles in order to stabilize the silver nanoparticles. Furthermore, SAMs assist efficient immobilization of PmB molecules onto the biosensor surface.

We chose LSPR method for many reasons: 1.LSPR based biosensors can be used in the extreme miniaturized scale(25), because in LSPR biosensors, every sensing site is as big as the spectrometer light emitted to the surface of nanostructures (which is a circle with 2mm radius in the present work). 2.Despite electrochemical biosensors, these sensors are not affected by ionic properties of sample solutions, so they are convenient for biological samples and clinical usages(26). 3.In LSPR biosensors, the interaction between sensing element and analyte, per se, leads to a signal transduction, so we do not need any labeling procedure which is cumbersome and time consuming. 4.To our knowledge, this would be the first step in using refractive index LSPR biosensors for detection of endotoxin. Therefore, the feasibility and advantages of this method for endotoxin detection would be explored for the first time.

Experimental Section

Materials

High purity silver granules(99.99%), 3-Mercaptopropionic acid(MPA), 1-Ethyl-3-[3-dimethylaminopropyl]carbodiimide hydrochloride(EDC) and N-hydroxysuccinimide(NHS) were purchased from Merck(KGaA Darmstadt, Germany). Lyophilized LPS from *E.Coli* O111:B4, polymyxin B sulfate salt(PmB) and phosphate-buffered saline(PBS) were obtained from Sigma-Aldrich. Hepatitis B surface antigen (HBs ag), lyophilizedLPS from *B. abortus* and pyrogen free water were procured from the Research and Production Complex of Pasteur Institute of Iran (Karaj, Iran). To minimize the influence of environmental conditions, most of the experiments were performed under a laminar flow hood.

UV-Visible Spectroscopy

After each step of surface modification, the substrates were washed by pyrogen free water consecutively in order to remove unbound molecules. Then they were immediately dried under N_2 stream (So from now on, we don't mention the washing and drying steps after each step of surface modification). After drying, the extinction spectra of substrates in air were taken from 200 to 800nm using a UV-visible spectrometer and the LSPR peak wavelengths were collected. The spectrometer light was emitted perpendicularly onto the substrates' surface.

Silver Nanocolumn Deposition on Glass Substrates

Microscope cover glass slides(QC Lab) were cut into 0.7cm × 2.7 cm pieces using a diamond pen and cleaned by piranha solution(H_2SO_4:H_2O_2=3:1) at 80 °C for 30min. Then, the glass substrates were washed by copious amounts of water and dried under N_2 stream.

The deposition of silver nanocolumns on glass substrate was performed by GLAD method using a custom designed thermal evaporation system(27). Deposition parameters including deposition rate, deposition thickness, azimuthal rotation speed, and glancing angle were fixed at 0.1 nm/s, t=400nm, φ=2rpm and, Θ=84° respectively, and the refractive index sensitivity of produced nanostructures was 134 nm/RIU. These parameters were chosen according to our coworkers' recent published paper in which they investigated and optimized effects of different deposition parameters on sensing properties of silver nanocolumns(28).

SAM Formation and PmB Immobilization

After formation of silver nanocolumns on the glass substrates, they should be stabilized by a SAM. For this purpose, the silver nanocolumn substrates were incubated in a 1mM ethanolic solutions of MPA for 2h. Afterwards, the substrates were incubated in 1:1 solutions of EDC 45mM and NHS 20mM in PBS(10mM, pH=6.5) for 1h in order to activate the carboxylic acid groups of SAM. Then SAM coated substrates were immersed in 1mL of 100µg/mL solutions of PmB in PBS for 1h.

Sample Preparation and Detection of endotoxin

Lyophilized endotoxin was dissolved in PBS buffer, and different concentrations of endotoxin solutions were provided. Endotoxin molecules have a natural tendency to aggregate. This would probably reduce the homogeneity of endotoxin samples. To solve this problem, endotoxin samples were sonicated at 50°C for 15 min and then vortexed vigorously for 5 min just before use. Then the PmB-immobilized substrates were exposed to 1 mL of endotoxin solutions in different concentrations for 1h. Finally, LSPR peak wavelength of each substrate was measured after endotoxin interaction with PmB. The difference between this LSPR peak wavelength and the LSPR peak wavelength of PmB-immobilized substrate was reported as $\Delta\lambda_{max}$.

The schematic diagram related to all the surface modification procedures is shown in fig. 1.

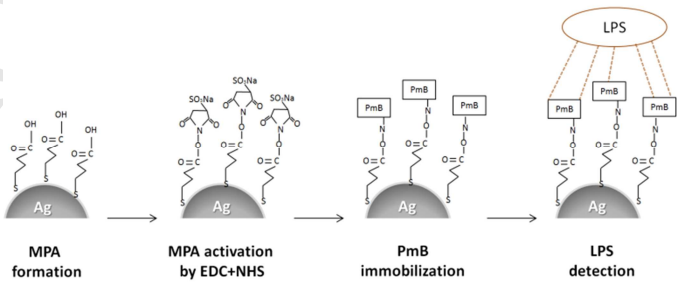

Fig.1- Schematic diagram related to different steps of surface preparation for LSPR detection of LPS molecules.

Stability Studies

Stability of silver-nanocolumn substrates made by GLAD method is a significant challenge that should have been well studied and improved. We used SAM of 1mM MPA solution in order to stabilize silver nanocolumns. To investigate effect of SAM on the stability of silver-nanocolumns, a bare silver nanocolumn substrate and a SAM-functionalized substrate were immersed in PBS solution for 24h. Then the LSPR spectra of each substrate in PBS solution were collected at special time steps during this 24h.

Results and Discussions

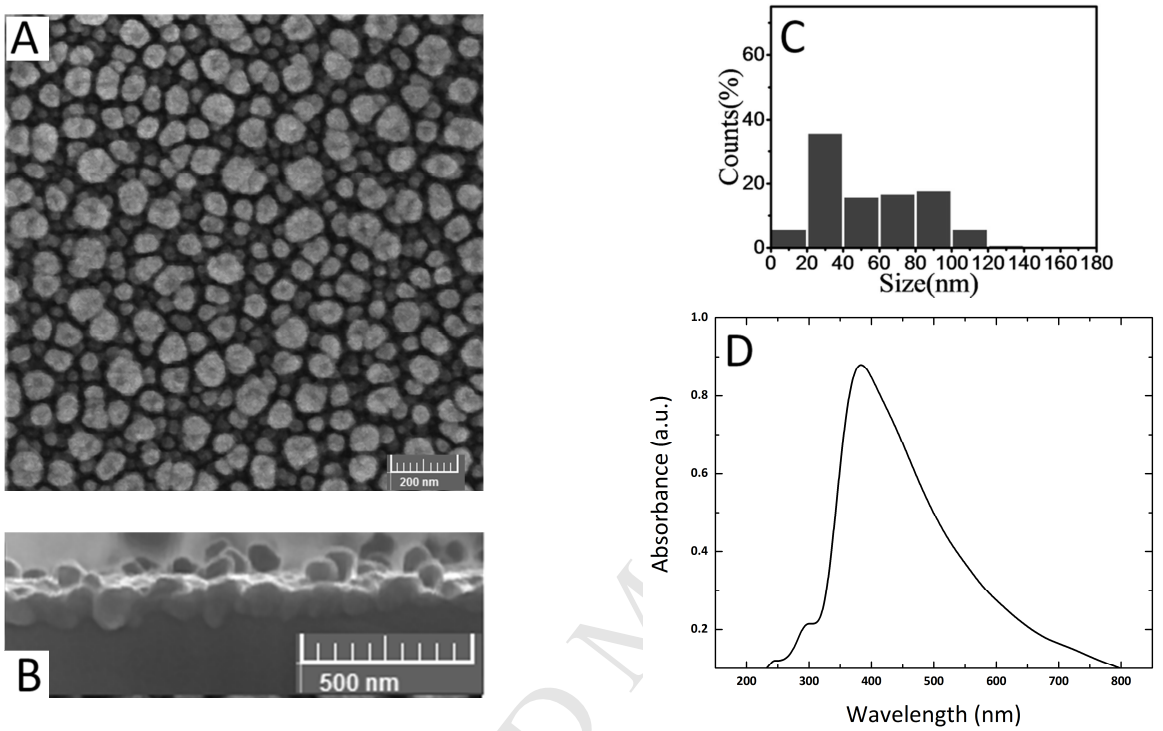

Fig. 2- Top-view SEM image (A), cross-view SEM image (B), histograms of diameter distribution (C) and absorbance spectra of silver nanocolumns. Nanostructures herein were prepared by GLAD method while the deposition rate, deposition thickness, azimuthal rotation speed, and glancing angle were fixed at 0.1 nm/s, t=400nm, ϕ=2rpm and, Θ=84° respectively.

As we discussed, GLAD method was used to produce silver nanostructures on glass surface. Fig.2 shows typical SEM images and size distributions of fabricated nanostructures(A,B,C). The inset in this figure illustrates the top view SEM image. As shown in this figure, an array of Ag nanocolumns with semi-spherical cross section is formed on the substrate. Based on the histograms of size distributions, the nanocolumns have the diameters ranging between 10 to 120 nm. The UV-Vis absorbance spectra of fabricated Ag nanostructures is also shown in fig. 2 (D). The Ag nanocolumns exhibit a strong plasmonic peak around wavelength of 382nm with width of 126 nm, which is suitable for sensing experiments based on our coworkers' previous results[28].

In LSPR biosensing, nanostructures with same morphology and homogeneity have the same optical characteristics such as refractive index sensitivity. Therefore, the more uniform nanostructures lead to the more reproducible and reliable results(29). In order to evaluate the reproducibility of silver nanostructures fabricated by GLAD method, we chose 8 different substrates randomly and checked the LSPR spectra of each sample. The data provided in table 1 indicate that these silver nanostructures are considerably reproducible. As it is demonstrated, different samples have almost same LSPR peak wavelength which is located in a small range of 380 to 385 nm.

Table 1- Reproducibility of silver nanocolumn substrate between 8 different samples

Sensor	1	2	3	4	5	6	7	8
λ_{max}(nm)	383.12	382.45	384.11	381.78	382.11	380.78	381.78	382.11
Absorbance at λ_{max}(a.u.)	0.8871	0.9321	0.8931	0.8937	0.9368	0.9143	0.9111	0.9371

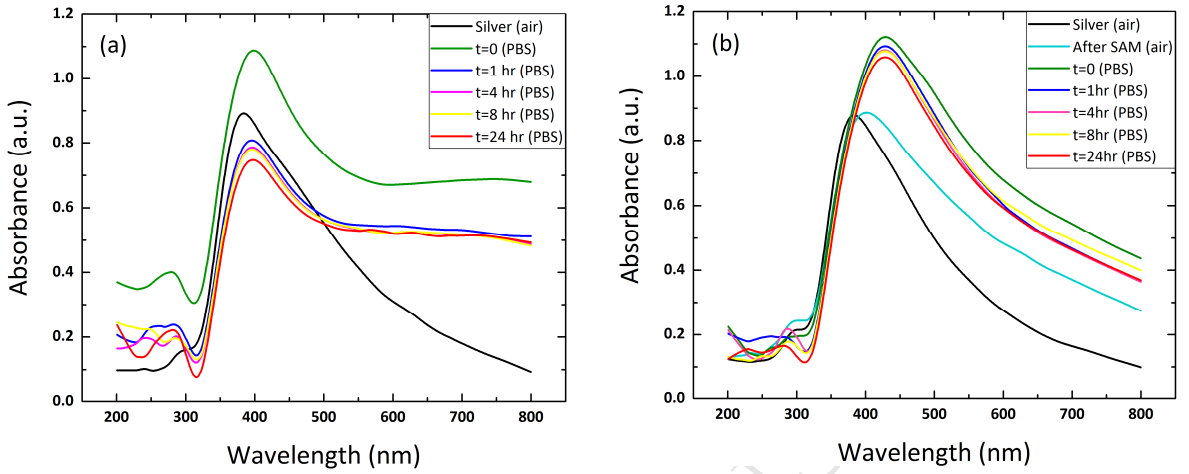

Fig.3- UV-visible spectra of bare silver-nanocolumn substrate(a), and SAM-functionalized substrate (b), before and after immersing in PBS solution for various incubation times.

Stability

In biosensing applications, nanostructures usually are immersed in solvents for long incubation time from 1 to 24 h. On the other hand, any change in the structure of nanoparticles would lead to a change in LSPR peak. Therefore, especially in LSPR biosensing, silver-based biosensor should be stable against oxidation and nanoparticle detachment in aqueous environments.

Fig. 3-a shows the extinction spectra of a silver nanocolumn substrate in PBS solvent during 24h. We chose PBS instead of water, for it is a closer emulate of physiological fluids. As it is demonstrated in fig. 3-a, at first moment of incubation, both LSPR peak wavelength and intensity of spectra increased due to the bigger refractive index of PBS environment compared to air. After 1h of incubation, there is a notable reduction in peak intensity, and also a blue shift about 8nm has been occurred in LSPR peak wavelength. This blue shift is due to the oxidation of silver nanoparticles in aqueous phase(30). Finally after 24h incubation, the reduction in peak intensity goes up to 32% while the position of LSPR peak wavelength is almost constant compared to t=1h. This reduction in peak intensity is probably because of detachment of silver nanoparticles from the surface of biosensor(23). The refractive index sensitivity of biosensor is also degraded from 134 to 76nm/RIU after 24h.

As it has been mentioned, we used SAM of 1mM MPA solution in order to stabilize the silver nanocolumns. The effect of SAM immobilization on stability of biosensor is shown in fig. 3-b. After 2h incubation in MPA solution, there is a redshift in LSPR spectra of substrate in air environment. This redshift is because of interaction of MPA molecules with silver surface. Herein after 24h of incubation of MPA-modified substrate inPBS solution, only about 5% reduction of peak intensity has been occurred. In addition, almost no blue shift in LSPR peak was observed after 24h. Therefore, SAMs of MPA have a remarkable influence on the stability of these biosensors, and by using them we can considerably protect silver nanoparticles from oxidation and detachment. Moreover, in this situation, general shape of LSPR spectra is almost constant and the refractive index sensitivity of biosensor slightly reduced from 134 to 119 nm/RIU after 24h.

Surface Modification and Endotoxin Detection

The LSPR spectra was measured after each step of surface modification. Fig. 4 shows the LSPR spectra of each step of surface modification for detection of 10 µg/ml endotoxin *E.coli* solution. In fig. 4-A, the LSPR peak wavelength of the silver nanocolumn substrate was λ_{max}= 382.80nm. After SAM formation (by MPA) and activation (by EDC and NHS) the peak wavelength was measured to be λ_{max}=406.92 nm (fig 4-B). After that, the substrate was incubated in PmB solution. Fig. 4-C illustrates the LSPR spectra after this step with peak wavelength of λ_{max}=421.03 nm. Then, the biosensor was prepared to detect endotoxin molecules. In this step, the sensor was exposed to 10 µg/ml endotoxin *E.coli*

solution. Fig. 4-D indicates the LSPR spectra related to this step. As we see, in this step the 31.21nm red shift was happened; consequently, the maximum wavelength was λ_{max}=452.24 nm.

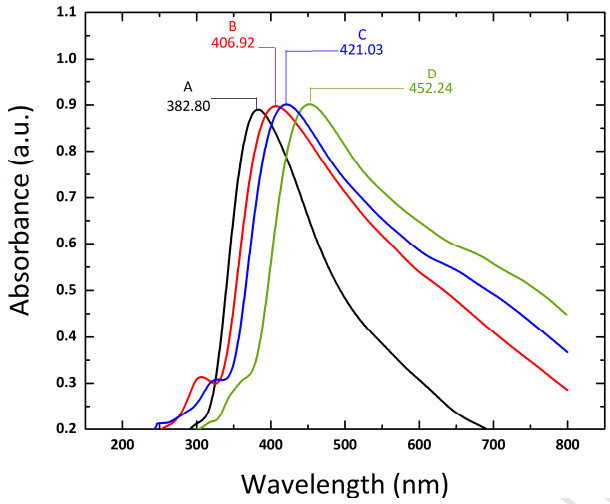

Fig 4- LSPR spectra representing the response of PmB-immobilized substrate to 10 µg/ml solution of endotoxin E.coli. (A) Silver nanocolumns, λ_{max}=382.80 nm. (B) Silver nanocolumns after formation of SAM of 1mM MPA and modification with EDC 45mM and NHS 20mM, λ_{max}=406.92 nm. (C) SAM coated substrate after immobilization of 100 µg/ml PmB solution, λ_{max}=421.03 nm. (D)PmB immobilized substrate after exposure to 10 µg/ml solution of endotoxin E.coli, λ_{max}=452.24 nm.

Negative control experiments also were performed for each step of surface modification. For example, fig. 5 demonstrates the LSPR spectra related to the control experiment of PmB immobilization. For this purpose, SAM functionalized substrate was incubated in 10µg/ml solution of endotoxin E.coli. After 1h, only 1.34nm blue shift is observed which is negligible. This result shows that in the absence of PmB molecules, the sensor would not detect endotoxin E.coli. In other words, it implies that redshift observed in fig. 4-D is due to the interaction of endotoxin molecules with just PmB molecules, and interaction of endotoxin with other areas of the surface is negligible.

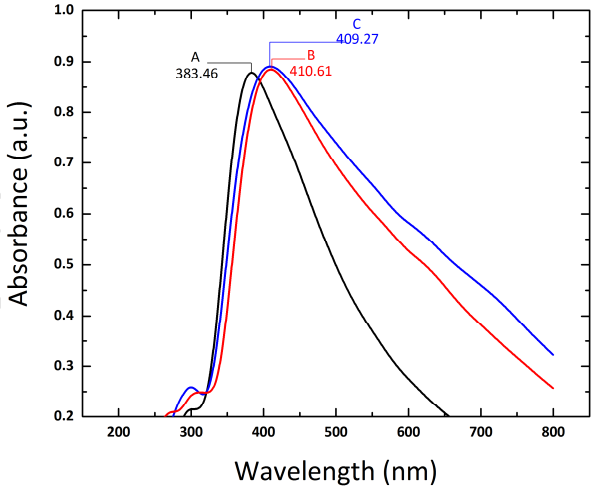

Fig. 5- LSPR spectra illustrating the response of SAM-coated substrate to 10 µg/ml endotoxin *E.coli* solution in absence of PmB molecules. (A) Silver nanocolumns, λ_{max}=383.46 nm. (B) Silver nanocolumns after formation of SAM of 1mM MPA and modification with EDC 45mM and NHS 20mM, λ_{max}=410.61 nm. (C)SAM immobilized substrate after exposure to endotoxin solution, λ_{max}=409.27 nm.

LOD Studies

Endotoxin *E.coli* solutions with different concentrations were exposed to the biosensors and the calibration curve was obtained (fig. 6).

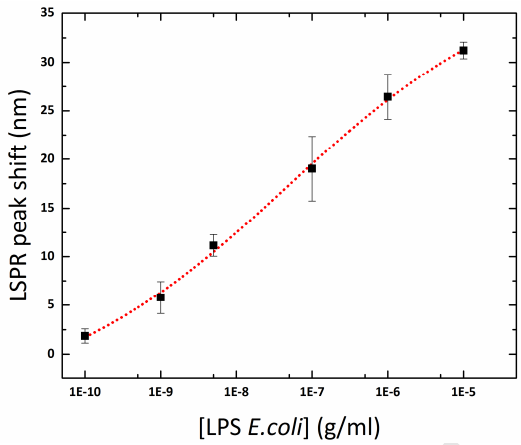

Fig. 6- Calibration curve of endotoxin *E.coli*- PmB binding at the surface of silver nanocolumn LSPR biosensor. The curve is fitted by sigmoidal curve fit (Hill1 Type) while R^2=0.99841. The error bars demonstrate the standard deviation from 3 independent measurements.

Calibration curve is fitted by a sigmoidal curve fit (Hill1 Type) while the coefficient of determination is measured to be R^2=0.99841 that demonstrates an excellent fitting. As it is represented in calibration curve (fig. 6), this biosensor shows response even to 100 pg/ml solutions of endotoxin E.coli, but we calculate the limit of detection (LOD) of biosensor by EC10 value. According to this method, 10% value of maximum signal is the signal related to the minimum detectable concentration. So LOD is measured to be 340 pg/ml for this biosensor. Table 2 represents that the LOD attained by this biosensor is acceptable and in most cases better than the other PmB-based endotoxin biosensors.

Table 2- Minimum limit of detection of different PmB-based endotoxin biosensors

Detection Method	Sensing Element	LOD (ng/ml)	Reference
Electrochemical (CV)	PmB	32.89×10^3	(12)
Electrochemical (EIS)	PmB	100	(31)
Fiber optic	PmB	10	(18)
LSPR	PmB	0.34	This study
Electrochemical (EIS)	PmB	0.2	(7)

Selectivity Studies

We investigated non-specific binding interactions in 2 sections:

1.Incubating PmB functionalized substrates in BSA and HBs-ag solutions: In order to understand whether PmB molecules are selective sensing element for endotoxin or not, two PmB-coated substrates were immersed in 10µg/ml solution of BSA and HBs-ag. BSA is usually chosen as a conventional protein in biological solutions. We also chose HBs-ag, because it is one of the biopharmaceutical products of Recombinant Biopharmaceutical Production Department of Institute Pasteur which must be tested for pyrogenic activity before injection. Therefore, we should have assured that our sensing element (PmB) has much less affinity to HBs-ag than endotoxin. Fig. 7 illustrates biosensor response to these proteins. After exposing BSA and HBs-ag to 2 different substrates, respectively 0.23nm and 0.58 nm LSPR peak shift was observed. These values are under the EC10 value of biosensor (3.96 nm), and it shows that our biosensor selectively interacts with endotoxin molecules compared to these protein species.

2.Incubating PmB functionalized substrate in a solution of endotoxin *B. abortus*: In this part, the biosensor was exposed to 10µg/ml solution of endotoxin of *B.abortus* bacteria in PBS. We chose endotoxin of *B.abortus* bacteria, because it is the second type of endotoxin contamination in our target sample (HBs-ag solution). After 1h incubation, 7.60nm LSPR peak shift was occurred (Fig. 7).
This quantity shows that our biosensor and probably other PmB-based biosensors are not highly selective for endotoxin

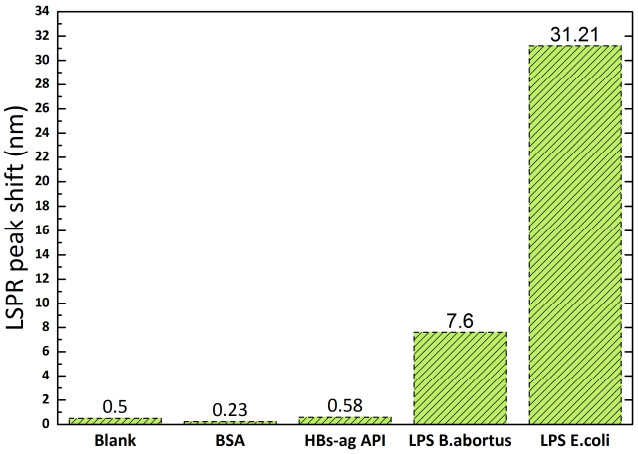

Fig. 7- Selectivity of PmB immobilized LSPR biosensor to some biological species. Concentration of all samples here is 10µg/ml and blank refers to PBS solution devoid of endotoxin as a control experiment.

molecules of a desired bacterial specie. Most of the published articles about endotoxin biosensors didn't consider this challenge of detecting different species of endotoxin. However, there are scarce articles in literature in which they showed these biosensors would not be selective between different endotoxins (3, 32), or they designed a selective biosensor to endotoxin of different bacterial species(33).
We also found out that there is a notable difference in biosensor response to endotoxin *B.abortus* and endotoxin *E.coli* at same concentrations. As it is demonstrated in fig 8, endotoxin *B.abortus* sample with same concentration shows lower tendency than endotoxin *E.coli* to interact with PmB molecules. We can bring a couple of reasons to explain this difference: 1.endotoxin *B.abortus* molecules have more fatty acid chains with longer chains and it makes them more stable against polycationic peptides(34). 2.anionic groups of endotoxin *B.abortus* are not completely accessible due to its specific molecular structure(35).
Overall, in this section we found out that by using this biosensor, not only can we detect endotoxin *E.coli*, but we also are able to detect second type of endotoxin contamination (endotoxin *B.abortus)* in our target samples. However, it should be emphasized that this biosensor is not selective between these 2 types of endotoxins, and probably by employing some other biorecognition element this problem will be solved too.

Conclusions

In this paper, we used an LSPR biosensor for detection of endotoxin. In order to overcome the instability of silver nanostructures, we used a SAM of MPA and minimized oxidation and detachment of silver nanostructures. This biosensor was able to detect endotoxin molecules with a detection limit of 340 pg/ml(˜3EU/ml). Furthermore, we performed some selectivity experiments and demonstrated that this biosensor can selectively detect endotoxins compared to other biological species. Therefore, this paper proposes a refractive index LSPR biosensor for quantitative detection of endotoxins, which is facile, label-free and sensitive.

Acknowledgements

We are grateful to our other coworkers at the Recombinant Biopharmaceutical Production Department of Institute Pasteur for their expert assistance.

References

1. Magalhães PO, Lopes AM, Mazzola PG, Rangel-Yagui C, Penna T, Pessoa Jr A. Methods of endotoxin removal from biological preparations: a review. J Pharm Pharm Sci. 2007;10(3):388-404.
2. Cohen J. The immunopathogenesis of sepsis. Nature. 2002;420(6917):885-91.
3. Lim SK, Chen P, Lee FL, Moochhala S, Liedberg B. Peptide-assembled graphene oxide as a fluorescent turn-on sensor for lipopolysaccharide (endotoxin) detection. Analytical chemistry. 2015;87(18):9408-12.
4. Limbut W, Hedström M, Thavarungkul P, Kanatharana P, Mattiasson B. Capacitive biosensor for detection of endotoxin. Analytical and bioanalytical chemistry. 2007;389(2):517-25.
5. Priano G, Pallarola D, Battaglini F. Endotoxin detection in a competitive electrochemical assay: synthesis of a suitable endotoxin conjugate. Analytical biochemistry. 2007;362(1):108-16.
6. Kato D, Iijima S, Kurita R, Sato Y, Jia J, Yabuki S, et al. Electrochemically amplified detection for lipopolysaccharide using ferrocenylboronic acid. Biosensors and Bioelectronics. 2007;22(7):1527-31.
7. Ding S-J, Chang B-W, Wu C-C, Chen C-J, Chang H-C. A new method for detection of endotoxin on polymyxin B-immobilized gold electrodes. Electrochemistry communications. 2007;9(5):1206-11.
8. Heras JY, Pallarola D, Battaglini F. Electronic tongue for simultaneous detection of endotoxins and other contaminants of microbiological origin. Biosensors and Bioelectronics. 2010;25(11):2470-6.
9. Yeo TY, Choi JS, Lee BK, Kim BS, Yoon HI, Lee HY, et al. Electrochemical endotoxin sensors based on TLR4/MD-2 complexes immobilized on gold electrodes. Biosensors and Bioelectronics. 2011;28(1):139-45.
10. Cho M, Chun L, Lin M, Choe W, Nam J, Lee Y. Sensitive electrochemical sensor for detection of lipopolysaccharide on metal complex immobilized gold electrode. Sensors and Actuators B: Chemical. 2012;174:490-4.
11. Kim SK, Hesketh PJ, Li C, Thomas JH, Halsall HB, Heineman WR. Fabrication of comb interdigitated electrodes array (IDA) for a microbead-based electrochemical assay system. Biosensors and Bioelectronics. 2004;20(4):887-94.
12. Zuzuarregui A, Arana S, Pérez-Lorenzo E, Sánchez-Gómez S, Martínez de Tejada G, Mujika M. Novel fully-integrated biosensor for endotoxin detection via polymyxin B immobilization onto gold electrodes. Journal of Sensors and Sensor Systems. 2013;2(2):157-64.
13. Zuzuarregui A, Souto D, Pérez-Lorenzo E, Arizti F, Sánchez-Gómez S, de Tejada GM, et al. Novel integrated and portable endotoxin detection system based on an electrochemical biosensor. Analyst. 2015;140(2):654-60.
14. Inoue KY, Takahashi S, Ino K, Shiku H, Matsue T. Development of an electrochemical Limulus amebocyte lysate assay technique for portable and highly sensitive endotoxin sensor. Innate immunity. 2012;18(2):343-9.
15. Su W, Lin M, Lee H, Cho M, Choe W-S, Lee Y. Determination of endotoxin through an aptamer-based impedance biosensor. Biosensors and Bioelectronics. 2012;32(1):32-6.
16. Su W, Kim S-E, Cho M, Nam J-D, Choe W-S, Lee Y. Selective detection of endotoxin using an impedance aptasensor with electrochemically deposited gold nanoparticles. Innate immunity. 2013;19(4):388-97.
17. Hreniak A, Maruszewski K, Rybka J, Gamian A, Czyżewski J. A luminescence endotoxin biosensor prepared by the sol–gel method. Optical Materials. 2004;26(2):141-4.
18. James E, Schmeltzer K, Ligler F. Detection of endotoxin using an evanescent wave fiber-optic biosensor. Applied biochemistry and biotechnology. 1996;60(3):189-202.
19. Noda K, Goto H, Murakami Y, Ahmed ABF, Kuroda A. Endotoxin assay by bioluminescence using mutant firefly luciferase. Analytical biochemistry. 2010;397(2):152-5.
20. Zeng L, Wu J, Dai Q, Liu W, Wang P, Lee C-S. Sensing of bacterial endotoxin in aqueous solution by supramolecular assembly of pyrene derivative. Organic letters. 2010;12(18):4014-7.
21. Wu J, Zawistowski A, Ehrmann M, Yi T, Schmuck C. Peptide functionalized polydiacetylene liposomes act as a fluorescent turn-on sensor for bacterial lipopolysaccharide. Journal of the American Chemical Society. 2011;133(25):9720-3.
22. Thompson M, Blaszykowski C, Sheikh S, Romaschin A. A true theranostic approach to medicine: Towards tandem sensor detection and removal of endotoxin in blood. Biosensors and Bioelectronics. 2015;67:3-10.
23. Gish DA, Nsiah F, McDermott MT, Brett MJ. Localized surface plasmon resonance biosensor using silver nanostructures fabricated by glancing angle deposition. Analytical chemistry. 2007;79(11):4228-32.
24. Kalita P, Dasgupta A, Sritharan V, Gupta S. Nanoparticle–Drug Bioconjugate as Dual Functional Affinity Ligand for Rapid Point-of-Care Detection of Endotoxin in Water and Serum. Analytical chemistry. 2015;87(21):11007-12.
25. Acimovic SS, Ortega MA, Sanz V, Berthelot J, Garcia-Cordero JL, Renger J, et al. LSPR chip for parallel, rapid, and sensitive detection of cancer markers in serum. Nano letters. 2014;14(5):2636-41.
26. Lee J-H, Kim B-C, Oh B-K, Choi J-W. Highly sensitive localized surface plasmon resonance immunosensor for label-free detection of HIV-1. Nanomedicine: Nanotechnology, Biology and Medicine. 2013;9(7):1018-26.
27. Sobhkhiz N, Moshaii A. Silver conical helix broadband plasmonic nanoantenna. Journal of Nanophotonics. 2014;8(1):083078-.
28. Abbasian S, Moshaii A, Vayghan NS, Nikkhah M. Ag Nanostructures Produced by Glancing Angle Deposition with Remarkable Refractive Index Sensitivity. Plasmonics. 2016:1-10.

29. Hammond JL, Bhalla N, Rafiee SD, Estrela P. Localized surface plasmon resonance as a biosensing platform for developing countries. Biosensors. 2014;4(2):172-88.
30. Fu J-X, Collins A, Zhao Y-P. Optical properties and biosensor application of ultrathin silver films prepared by oblique angle deposition. The Journal of Physical Chemistry C. 2008;112(43):16784-91.
31. Rahman MSA, Mukhopadhyay SC, Yu P-L, Goicoechea J, Matias IR, Gooneratne CP, et al. Detection of bacterial endotoxin in food: New planar interdigital sensors based approach. Journal of Food Engineering. 2013;114(3):346-60.
32. Oliveira MD, Andrade CA, Correia MT, Coelho LC, Singh PR, Zeng X. Impedimetric biosensor based on self-assembled hybrid cystein-gold nanoparticles and CramoLL lectin for bacterial lipopolysaccharide recognition. Journal of colloid and interface science. 2011;362(1):194-201.
33. Xie P, Zhu L, Shao X, Huang K, Tian J, Xu W. Highly sensitive detection of lipopolysaccharides using an aptasensor based on hybridization chain reaction. Scientific Reports. 2016;6.
34. Jarvis BW, Harris TH, Qureshi N, Splitter GA. Rough lipopolysaccharide from Brucella abortus and Escherichia coli differentially activates the same mitogen-activated protein kinase signaling pathways for tumor necrosis factor alpha in RAW 264.7 macrophage-like cells. Infection and immunity. 2002;70(12):7165-8.
35. Velasco J, Bengoechea JA, Brandenburg K, Lindner B, Seydel U, González D, et al. Brucella abortus and its closest phylogenetic relative, Ochrobactrum spp., differ in outer membrane permeability and cationic peptide resistance. Infection and immunity. 2000;68(6):3210-8.